Atmospheric Environment 216 (2019) 116924

Contents lists available at ScienceDirect

Atmospheric Environment

journal homepage: www.elsevier.com/locate/atmosenv

High cancer risk from inhalation exposure to PAHs in Fenhe Plain in winter: A particulate size distribution-based study

Hongyan Li[a], Hongyu Li[a], Lu Zhang[a], Mingchao Cheng[a], Lili Guo[a], Qiusheng He[a,*], Xinming Wang[b], Yuhang Wang[c]

[a] School of Environment and Safety, Taiyuan University of Science and Technology, Taiyuan, China
[b] State Key Laboratory of Organic Geochemistry, Guangzhou Institute of Geochemistry, Chinese Academy of Sciences, Guangzhou, China
[c] School of Earth and Atmospheric Science, Georgia Institute of Technology, Atlanta, GA, USA

ARTICLE INFO

Keywords:
Polycyclic aromatics hydrocarbons
Size distribution
Diagnostic ratios
Coefficient of divergence analysis
Health risk assessment

ABSTRACT

Fenhe Plain is a typical region polluted combinedly by coal combustion and coking activities with serious air pollution problem, especially in winter. In order to clarify the size distribution and health risk of polycyclic aromatic hydrocarbons (PAHs) in winter of the Fenhe Plain, the respirable aerosol particles (PM_{10}) were collected by cascade impactor, and 17 PAHs were analyzed. The results showed that the average mass concentration of PM_{10}-bound PAHs was 689.19 ng/m^3, which was higher than that in many other domestic and overseas cities. The particulate PAHs mainly distributed in the < 0.95 μm size range, accounting for more than 60% of the total. Under the combined influence of local emissions, low temperature, low intensity of solar radiation, dry atmosphere and Kelvin effect, naphthalene (Nap) displayed a bimodal distribution, while the rest of the 17 PAHs all followed a nearly unimodal size distribution. Wind and humidity were important factors which could influence the size distribution of PAHs. Coefficient of divergence (CD) analysis showed that PAHs between all of the sizes had a high spatial heterogeneity in source factor contributions, although diagnostic ratio indicated similar sources among them. Health risk assessment found that the lifetime cancer risk of exposure to particulate PAHs was 1693.76 parts per million people. Ultrafine particles (< 0.95 μm) predominated the total carcinogenicity of the particulate PAHs, while benzo(a)pyrene (BaP), dibenzo(a,h)anthracene (DahA), benzo(b)fluoranthene (BbF), benzo(a)anthracene (BaA), benzo(k)fluoranthene (BkF) and indeno(1,2,3-cd)pyrene (IcdP) were the major carcinogenic components. Traffic exhausts contributed most to the carcinogenic PAHs, followed by coal combustion and coking. Our study can provide reference for the pollution control and residential health protection in Fenhe Plain, and bring more reasonable parameterizations to the estimation of PAHs outflow from this key region to other international regions.

1. Introduction

Atmospheric PAHs are important organic contaminants in urban air being concerned widely because of their large emissions, complex sources, high persistence in the environment, as well as strong carcinogenic and mutagenic properties (Lv et al., 2016). Their emission mainly results from the incomplete combustion of carbon-containing materials, such as biomass, coal, petroleum, garbage, tobacco and charbroiled meat (Zhang et al., 2012). High levels of atmospheric PAHs have been demonstrated to increase the lung cancer risk (Boström et al., 2002) with incremental annual lung cancer risk being up to 6.5 per million people due to inhalation exposure to PAHs in China (Zhang et al., 2009).

As semi-volatile organic compounds, PAHs can partition between the gas and the particulate phase because of their relatively low vapor pressures (Wang et al., 2011). Previous studies showed that most of the PAHs are more apt to accumulate in the small particles than the large particles, especially in those with an aerodynamic diameter (Dp) below 10 μm, known as PM_{10} (Zhou et al., 2005; Zhu et al., 2014; Lv et al., 2016). Because such particles are inhalable and can deposit in the human respiratory system, the PM_{10}-bound PAHs can be released and contact with the tissue cells for a long time, and then cause great harm to human health (Zhang et al., 2012). The fine particles can even travel deep into the alveoli and, for the smallest particles, potentially enter the bloodstream, thus exposing people to both particles and particle-bound compounds (Geiser et al., 2005; Lv et al., 2016). Due to the partitioning

* Corresponding author.
E-mail address: heqs@tyust.edu.cn (Q. He).

https://doi.org/10.1016/j.atmosenv.2019.116924
Received 18 February 2019; Received in revised form 23 August 2019; Accepted 24 August 2019
Available online 28 August 2019

process and the deposition depth after inhalation strongly depends on particle size, the particle size distribution of PAHs plays a critical role in their health impacts. The distribution of high molecular mass PAHs is of particular importance, because most of them are carcinogenic and mainly exist in particle phase due to their very low vapor pressure (Akyuz and Cabuk, 2009; Wu et al., 2014). In addition, the size distribution of PAHs in particles can determine the transport distance and amount, dry deposition and wet precipitation fluxes, and lifetime of particulate PAHs at some extent (Kaupp and McLachlan, 1999).

A number of studies conducted in various countries and cities, as summarized by Lv et al. (2016), have documented that the size distribution of PAHs varies with their releasing sources, particle aging processes, and meterological conditions in different places. These studies were limited to large and developed metropolises in each country, i.e., Beijing (Zhou et al., 2005), Tianjin (Wu et al., 2006), Shanghai (Wang et al., 2016b), Xi'an (Ren et al., 2017) and the Pearl River Delta (Bi et al., 2005; Duan et al., 2007; Ren et al., 2017) in China, Athens (Theodosi et al., 2011), Heraclion (Kavouras and Stephanou, 2002), Island of Crete (Kavouras and Stephanou, 2002) and Thessaloniki in Greece (Chrysikou et al., 2009), Yokohama in Japan (Kameda et al., 2005), and six urban sites (Duisburg in Germany, Prague in Czech Republic, Amsterdam in The Netherlands, Helsinki in Finland, Barcelona in Spain and Athens in Greece) in Europe (Saarnio et al., 2008). The PAHs size distribution characteristics and related health risk in Fenhe Plain in China are still unknown.

Fenhe Plain in Shanxi province of China is one of the predominant PAHs emitting area in the world (Fig. 1a) and the most polluted province in North China because of its huge amount of coal combustion and coking activities without efficient emission control (Zhang et al., 2016). It has been reported that the emission density of PAHs in this province was three times of the Chinese average level and 13 times of the American level (Jiang et al., 2013). Maybe for this reason, the morbidity of lung cancer in Shanxi is very high (one time higher than the Chinese average level). The incidence of neural tube defects in Shanxi is called "the peak of Everest" for this disease in the world (Li et al., 2006), which has also been demonstrated to be related with women's high-level exposure to PAHs at some extent (Ren et al., 2011). Fenhe Plain is also the largest outflow region in China which contributes about 33% to the total outflow of BaP from China. It was found that although this region is farther from the eastern boundary of China, strong zonal winds at the lower troposphere associated with southward penetration of the polar front during the wintertime carry a large quantity of PAHs out of China (Zhang et al., 2011).

Due to the serious air pollution, Fenhe Plain has been listed as one of the national battlefields of "Blue Sky Defense" in 2018 by the Chinese Government. Before setting reasonable target for atmospheric PAHs control, the size distribution characteristics, accurate exposure level and health risk must be clear. However, many previous studies always considered the atmospheric PAHs concentration in particulate phase as the surrogate of exposure concentration in estimating the health risk of PAHs in particles (Wang et al., 2016b; Tomaz et al., 2016; Ren et al., 2017), but ignored the deposition efficiency of particles the PAHs bound to which are highly particle-size dependent. It will result in a very large overestimation of the risk as demonstrated by Luo et al. (2015). It is proposed that the outflow flux estimations of PAHs will also have large uncertainty when the size distribution characteristics of the aerosols are unclear (Zhang et al., 2011). However, current knowledge on PAHs size distribution in the Fenhe Plain remains unknown. To evaluate the health risk associated with PAHs exposure in Fenhe Plain accurately, and bring more reasonable parameterizations to the estimation of PAHs outflow from this key region to other international regions, we conducted a sampling campaign in winter to examine the size distribution of particle-bound PAHs and estimate the cancer risk of PAHs in this specific area. The potential sources and influences of meterological parameters on the size distribution were also analyzed. The acquired information is expected to provide a better understanding of the size-distribution characteristics and health risk of PAHs associated with coal combustion and coking activities.

2. Methods

2.1. Sample collection

Our sampling site was established in Taiyuan, which is a typical area of Fenhe Plain experiencing hazardous levels of pollution due to coal combustion and coking emissions. Detailed information about its topography, industrial distribution and meteorological characteristics has been described in our previous studies (Li et al., 2016). To investigate the average exposure levels of PM_{10} and associated PAHs for people in the investigated area and avoid the influence from ground-level emission sources like residential coal combustion and traffic near the sampling site, the sampling (Fig. 1b) was conducted on the roof (about 50 m high) of a sixteen-floor building on the campus of Taiyuan University of Science and Technology. In winter, most of the people like to stay indoors, while quite a lot of residence and office buildings have a height of about 100 m. Therefore, 50 m represents the intermediate height. Although outdoor concentration and indoor concentration cannot be equated, many evidences indicate that the difference

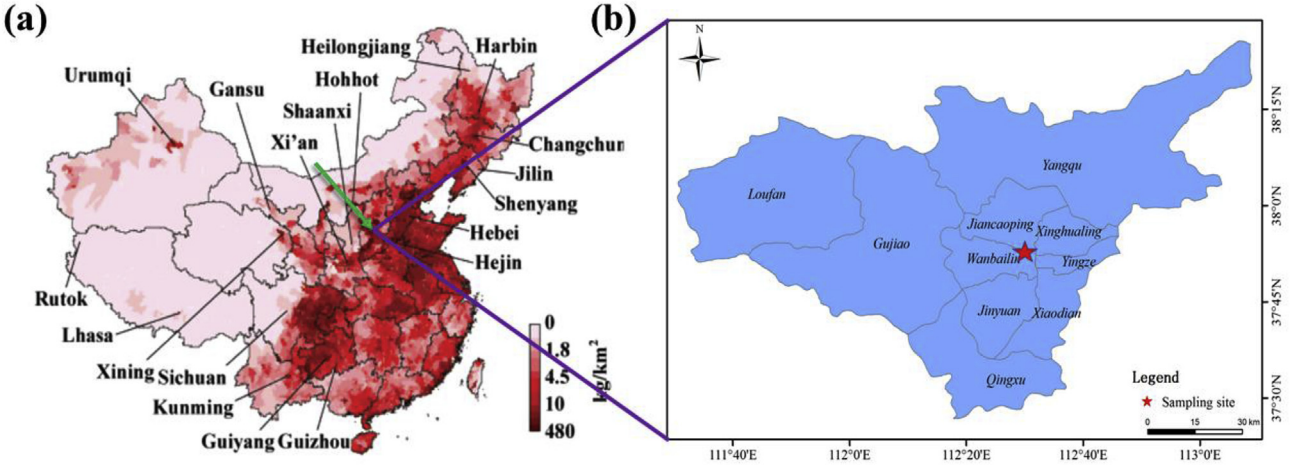

Fig. 1. (a) Location of the Taiyuan city (the greenarrow point to) and the PAHs emission density (g/km^2) in individual provinces and municipalities in 2004 (Zhang et al., 2007), (b) the location of the sampling site (marked with a red pentagram). (For interpretation of the references to color in this figure legend, the reader is referred to the Web version of this article.)

between them is not very large (Zhao et al., 2015; Wang et al., 2016a).

Size-segregated PM_{10} aerosol samples were collected for 20 days from December 14, 2014 to January 3, 2015. The representativeness and repeatability of the data from our sampling was discussed in the Text S1. The sampling duration was 24 h (from 8:00 a.m. to 8:00 a.m. of the next day). Airborne particles were collected using a TE-235 five-stage high-volume cascade impactor (made in the USA) at a flow rate of 0.565 m^3/min. The cascade impactor can fractionate suspended particulates into as many as five size fractions. Impactor cut-points are 10 (inlet), 7.2, 3, 1.5 and 0.95 μm, with the last stage collecting all particles smaller than 0.95 μm (backup filter). Quartz filters (Whatman QM-A, 20.3 × 25.4 cm) were used as a surrogate surface and placed on each impaction plate to collect the impacted particles of different sizes. Before use, the filters were baked at 500 °C for 4 h, equilibrated at 25 °C and 50% relative humidity for 48 h, and then weighed using a AB204-S micro-balance (METTLER company, Switzerland) accurate to 0.1 mg. After sampling, the membranes were equilibrated and weighed again using the same procedure. To ensure the accuracy, each filter were weighed at least four times before and after sampling, and the results were averaged. Then, the filters were wrapped in aluminum foil, and stored frozen at −20 °C until analysis.

Meteorological data including temperature, relative humidity, wind speed and wind direction were simultaneously recorded by Shanxi Provincial Meteorological Information Network with 60 min time resolution.

2.2. Extraction and analysis

One-fourth of each filter was cut into small pieces, spiked with recovery surrogate standards (naphthalene-d8, acenaphthene-d10, phenanthrene-d10, chresene-d12, perylene-d12), and extracted ultrasonically with dichloromethane (DCM) for 30 min with 3 replications. The combined organic extract was filtered, condensed to 1 mL by a rotary evaporator, and then cleaned-up by a silica-alumina column that was filled with 6 cm aluminum oxide, 12 cm silica gel, and 1 cm anhydrous Na_2SO_4. The cleanup column was eluted with 30 mL hexane and 30 mL DCM/hexane (1:1, v/v) in sequence. All the eluates were collected and condensed to below 1 mL through a rotary evaporator and a termovap sample concentrator. Hexamethylbenzene was added as the internal standard and the final volume of the sample was adjusted to 1 mL. Gas chromatography coupled to mass spectrometry (GC-MS, 2010 plus, SHIMADZU) was used for the separation and quantification of the target PAHs.

In this study, 17 PAHs were detected including Nap (2-ring), acenaphthylene (Acy, 3-ring), acenaphthene (Ace, 3-ring), fluoranthene (Flu, 3-ring), phenanthrene (Phe, 3-ring), anthracene (Ant, 3-ring), fluoranthene (Fla, 4-ring), pyrene (Pyr, 4-ring), BaA (4-ring), Chrysene (Chr, 4-ring), BbF (5-ring), BkF (5-ring), BaP (5-ring), IcdP (6-ring), DahA (5-ring), benzo[ghi]perylene (BghiP, 6-ring) and Coronene (Cor, 7-ring).

2.3. Quality assurance and quality control (QA/QC)

PAHs concentrations were quantified via calibration curves (internal standard method) constructed at six concentrations (0.025, 0.05, 0.1, 0.25, 0.5 and 1 ng/mL). The peaks of each PAH components were good, and the linear correlation coefficients were greater than 0.99. Procedural blanks, standard spiked blanks, and duplicate samples were analyzed for each set of 10 samples for quality assurance and control. PAHs were not detected in the procedural blanks. The mean recoveries of samples were: naphthalene-D8, 51.4%; acenaphthene-D10, 72.4%; phenanthrene-D10, 95.6%; chrysene-D12, 109%; and perylene-D12, 121%.

2.4. Methodology for inhalation exposure and cancer risk assessment

The detailed methods used to do the assessment of inhalation exposure, deposition efficiency and flux, as well as lifetime cancer risk were similar with those reported by Luo et al. (2015). The inhalable (IF), thoracic (TF), and respirable fractions (RF) of PM_{10}-bound PAHs are estimated respectively based on the criteria given by the International Standards Organization and American Conference of Governmental Industrial Hygienists (Hinds, 1999). The inhalable fraction represents the particles inhaled through the nose and/or mouth. The thoracic fraction represents the particles penetrating progressively into the lung. The respirable fraction represents the particles reaching beyond the gas exchange region. When assessing the deposition efficiency and flux, the respiratory system (RS) was divided into three main deposition regions: head airway (HA), tracheobronchial region (TR), and alveolar region (AR). The fractions of PM_{10}-bound PAHs deposited in the three regions were calculated with the simplified equations from the International Commission on Radiological Protection (ICRP) model (Hinds, 1999; International Commission on Radiological Protection, 1994).

The human incremental lifetime cancer risk (LCR) was assessed by:

$$LCR = \sum (C_{PAH} \times TEF_{PAH}) \times UR_{BaP}$$

where C_{PAH} is the deposition concentration of a specific PAH in the whole respiratory tract; TEF_{PAH} is the toxicity equivalency factor of PAH based on benzo[a]pyrene (Table S1), and UR_{BaP} is the unit relative risk of benzo[a]pyrene. In this study, the value of $8.7*10^{-5}$ per ng/m^3 for UR_{BaP} is used, which is from epidemiology studies on coke-oven workers over a lifetime of 70 years (World Health Organization, 2000).

3. Results and discussion

3.1. Pollution characteristics of PM_{10}-bound PAHs

To characterize the size distribution of PAHs in the PM_{10} samples in the winter of Fenhe Plain, we first determined the 24-h averaged concentrations of PM_{10} and PAHs bound to PM_{10}. As shown in Fig. 2c, the daily mass concentration of PM_{10} ranged from 76.04 to 349.82 μg/m^3. The average mass concentration was 199.10 μg/m^3, exceeding the Chinese 24 h Grade II standard (150 μg/m^3) according to China National Ambient Air quality Standard (NAAQS) (GB3095-2012) issued in 2012 by Ministry of Environmental Protection in China (MEP) and implemented in 2016 (MEP, 2012). The total PAHs (T-PAHs) mass concentration adsorbed on PM_{10} ranged from 52.00 to 1506.11 ng/m^3, with an average of 689.19 ng/m^3 (Fig. 2b). The average of 24-h average concentrations of T-PAHs bound to PM_{10} in Fenhe Plain was much higher than that in many other domestic and foreign cities, such as Xiamen (10.5 ng/m^3) (Hong et al., 2007), Beijing (85.36 ng/m^3) (Duan et al., 2012), Kuala Lumpur in Malaysia (6.28 ± 4.35 ng/m^3) (Omar et al., 2002), Teheran in Iran (148.43 ng/m^3) (Hoseini et al., 2016), Naples in Italy (urban traffic site, 6.03 ng/m^3) (Di Vaio et al., 2016), Zonguldak in Turkey (492.4 ng/m^3) (Akyüz et al., 2009), and Cordova in Argetina (5.266 ng/m^3) (Amarillo et al., 2017).

The high T-PAHs mass concentration bound to PM_{10} in the winter of Fenhe Plain could be ascribed to the large emissions of PAHs in winter from coal-related industries (especially the coking plants) along Fen river, residential coal combustion and traffic exhausts (Zhang et al., 2016; Li et al., 2016). The atmospheric conditions in winter also account for the high PAHs concentration in particles at some extent, because low temperature and low intensity of solar radiation favors the condensation and adsorption of PAHs on suspended particles that are present in urban air while slows down the PAHs photodegradation (Lv et al., 2016). The mean concentration of PAHs in PM_{10} in Fenhe Plain was lower than that of Lanzhou (1855.47 ng/m^3) in China (Yu et al., 2013), as well as Delhi in India (2293.02 ng/m^3) (Sharma et al., 2008)

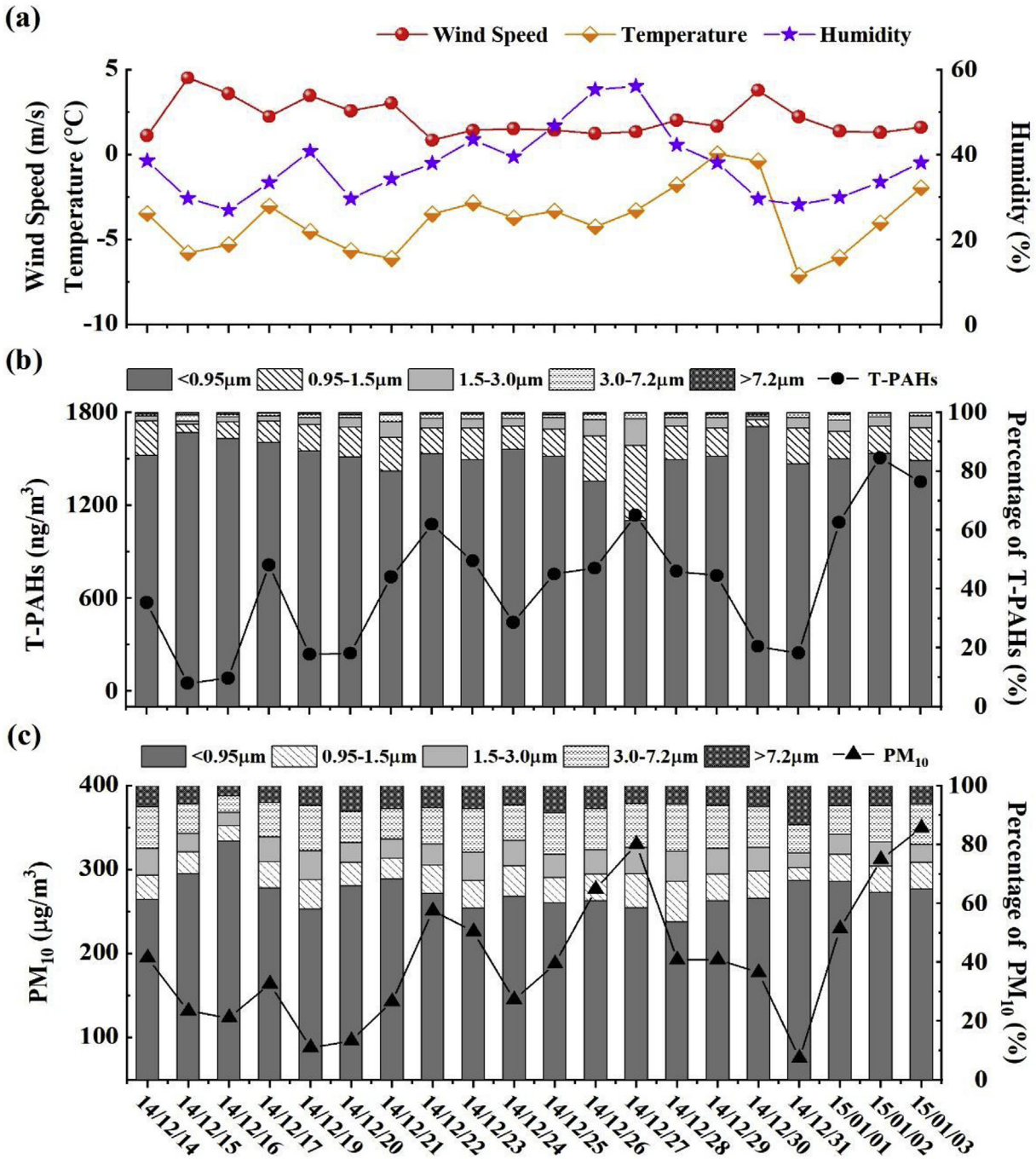

Fig. 2. The time series of meteorological parameters (temperature, wind speed and humidity) (a), T-PAHs concentrations (ng/m^3) (b), PM_{10} concentrations (μg/m^3) (c), and fractioned size composition in percentage of T-PAHs (b) and PM_{10} (c) during the sampling period.

due to different emission sources, emission strength, topography and meteorological conditions.

During the sampling period, the concentrations of PM_{10} and PAHs had the similar variation trends with strong positive correlation between them (R^2 = 0.88), suggesting like sources for them. Meantime, the size distribution profiles of PM_{10} and PAHs were also similar with < 0.95 μm being the dominant size fraction, accounting for 53.61%–81.19% and 63.19%–95.03% to the total PM_{10} and T-PAHs, respectively (Fig. 2b and c). The high enrichment of PM_{10} in small particle size indicates the important roles of anthropogenic origins (e.g., vehicles and coal combustion) (Lv et al., 2016; Theodosi et al., 2011). According to Whitby's viewpoint, fine particles (Dp < 2 μm) are produced predominantly from gas to particle conversion and from incomplete combustion (Whitby et al., 1972). Take the aerosol samples from coke enterprises as an example, it was found that $PM_{1.4}$ and $PM_{2.1}$ accounted for > 77% and > 86% of the total particulates, respectively (Mu et al., 2017). In coal combustion emissions, more than 77% of the total was found to be fine PM fraction with size less than 2.5 mm ($PM_{2.5}$) (Shen et al., 2010a,b). The smaller size particles have bigger specific surface area, and so can adsorb or absorb more PAHs. Therefore, the enrichment of T-PAHs in < 0.95 μm particle size was also the highest.

The proportions of combustion-derived PAHs (COMPAHs: Flu, Pyr, Chr, BbF, BkF, BaA, BaP, IcdP and BghiP (Wang et al., 2016b) and carcinogenic PAHs (CANPAHs: BaA, BbF, BkF, BaP and IcdP (Wang et al., 2016b) in the total PAHs in different size ranges are shown in

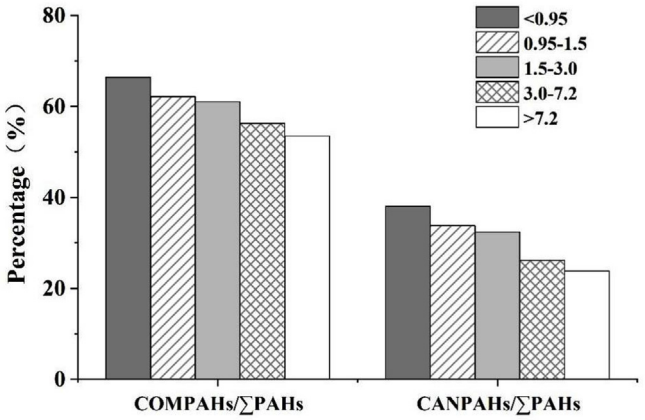

Fig. 3. The percentages of combustion-derived PAHs (COMPAHs) and carcinogenic PAHs (CANPAHs) in the total PAHs in different size ranges.

Fig. 3. As the decrease of the particle size, the contributions of these two groups of PAHs both increased. The total concentration of COMPAHs accounted for 53.47%–66.42% of the total PAHs in each size range, indicating that combustion source should be the major source of PAHs in the winter season of Fenhe Plain. The mass percentage of CANPAHs to T-PAHs in the five size fractions ranged from 23.82% to 38.00%. The data obtained in this study were lower than that from other studies: Wang et al. (2015) in Zhengzhou city of China (> 50% in $PM_{2.5}$), He et al. (2014) in Nanjing city of China (49.24–64.51%), Bourotte et al. (2005) in Saõ Paulo city of Brazil (50%); higher than that of Kaur et al. (2013) in Amritsar of India (12%); while similar with that of Kong et al. (2010) in Liaoning Province of China (29%); Hong et al. (2007) in Xiamen of China (28%); Zhu et al. (2014) at the China Yellow River Delta National Nature Reserve (27%). BaP is a strong carcinogenic monomer and its concentration has been utilized to indicate the potential health risk of PAHs to human beings (Saarnio et al., 2008). Many countries and cities have established corresponding ambient air quality standards for this compound. The Chinese daily standard value of BaP is 2.5 ng/m^3 (MEP, 2012). In this study, the average mass concentration of BaP was 42.54 ng/m^3, about 17 times of the standard limit. The World health organization (WHO, 2000) recommended more stringent BaP daily reference residential value of 1 ng/m^3. This indicates that the pollution level in the winter of Fenhe Plain is really serious and may be a threat to the health of local residents.

3.2. Size distribution characteristics of PAHs

As shown in Fig. 4a, along with the increase in particulate size, the distribution ratios of low molecular weight (LMW) PAHs (2, 3-ring PAHs) also increased, oppositely, the ratios of high molecular weight (HMW) PAHs (5, 6, 7-ring PAHs) decreased. The distribution ratios of medium molecular weight (MMW) PAHs had no significant difference among different size ranges. The results are similar in different cities (Wang et al., 2016b; Ren et al., 2017) due to the fact that less volatile PAH species preferentially condense on fine particles and more volatile ones are inhibited on smaller particles because of the Kelvin effect (Hien et al., 2007; Keshtkar and Ashbaugh, 2007). Although the distribution ratio of low ring number PAHs in coarse particles was higher than that in fine particles, all the PAH compounds were mainly concentrated in < 0.95 μm particle size range, followed by the range of 0.95–1.5 μm (Fig. 4b). Except for Nap, the proportions of other PAH compounds in the size range of < 0.95 μm were up to 80% or more (Fig. 4b).

To better characterize the size distribution of PM_{10} and PAHs, we plotted a histogram of the relative mass of dC/dlogDp versus the Dp on the logarithmic scale, which is an useful method for comparing the contributions of coarse and fine particles to the PAHs concentrations (Zhu et al., 2014). As shown in Fig. 5, the PM_{10} and Nap which has 2 rings exhibited a bimodal distribution. The major peaks for PM_{10} were in the ranges of < 0.95 (accumulation mode) and 3.2–7.2 μm (coarse mode), while those for Nap were in the ranges of 0.95–1.5 (accumulation mode) and 7.2–10 μm (coarse mode). The distribution type of Nap was similar with other reported results (Zhou et al., 2005; Wu et al., 2006). The remaining 16 PAHs all had a nearly unimodal particle size distribution type with the peak in the range of < 0.95 μm (accumulation mode) for Acy (3 ring), Ace (3 ring), and Cor (7 ring), and in the range of 0.95–1.5 μm for the rest. Different size distribution characterization of PAHs from PM_{10} indicates that the distribution of PM_{10} is not the controlling factor of the PAHs size distribution in Fenhe Plain.

The previous studies on the size distribution pattern of PAHs in source emissions showed that PAHs mainly exhibited an accumulation-mode-peak unimodal distribution with the peak being in fine particle size fraction (Shen et al., 2010, 2013; Liu et al., 2014; Mu et al., 2017). The size distribution pattern of PAHs in urban particles is always different from the source particles. Earlier urban studies found that LMW PAHs have a bimodal particle size distribution type which contains one mode peak in the accumulation size range (< 2.5 μm) and another mode peak in coarse size range (> 2.5 μm). As the number of PAHs' aromatic rings increases, the intensity of the accumulation-mode peak increases gradually, while the coarse-mode peak decreases and even disappears for five- and six-ring PAHs (Zhou et al., 2005; Duan et al., 2007; Lv et al., 2016). The species having the same molecular weight present similar distribution type in old air mass. This is due to that PAH compounds will experience repartitioning processes between gas and particle, or among different size particles after being released into the air. Both of the processes are controlled by the vapor pressure of PAHs, which are directly related to their molecular weight in general. Therefore, the longer the aging time, more obvious the relationship between the distribution type and the molecular weight. That is, PAH compounds with the same molecular weight and similar dipole moment have almost identical distributions with particle size (Venkataraman and Friedlander, 1994; Wu et al., 2006).

In this study, no bimodal distribution type except Nap was observed, and also no relationship between the distribution type and the molecular weight of PAHs. Oppositely, the distribution type of our aerosol samples is closer to that of the source samples, indicating that the PAHs may mainly arise from local fresh emissions, and do not attain equilibrium between particles of different size in the ambient air during short distance transport. Previous study reported that the shorter the distance to the source, the higher the portion of PAHs associated with fine particles (Bi et al., 2005; Chrysikou et al., 2009). In addition, low temperature and dry atmosphere conditions in winter of Fenhe Plain do not favor the growth of fine combustion-generated particles and the volatilization of PAHs from fine particles, which are important paths for PAHs to become associated with coarse particles (Wu et al., 2006; Liu et al., 2014).

The mass median diameter (MMD), the diameter that divides the total mass by two (Yang et al., 2005), was calculated using an equation provided by Kavouras and Stephanou (2002). In the samples of Fenhe Plain, the MMD value of PM_{10} ranged from 0.59 to 0.89 μm with an average of 0.75 μm, which was much lower than that in other cities such as Tianjin in China (1.84–1.88 μm) (Wu et al., 2006), Guangzhou in China (0.98 μm) (Bi et al., 2005) and Thessaloniki in northern Greece (1.26 μm) (Chrysikou and Samara, 2009). Our results suggest that the fine particle pollution in Fenhe Plain is very severe. The MMD values of the individual PAHs, which are lower than that of PM_{10}, were in the range of 0.53–0.59 μm except Nap (0.72). The values are higher than those of traffic exhausts (gasoline-powered cars, 0.45 μm; motorcycles, 0.15–0.42 μm) (Yang et al., 2005), a heavily trafficked roadside in southern Taiwan (~0.3 mm for total PAHs in the 0.01–10 mm size range (Lin et al., 2008)), and low caking coals (0.11–0.13 μm), but lower than those of biomass and coal combustion emissions (indoor crop residue burning, 0.96–1.5 μm; fuel wood, 0.75 μm; brushwood,

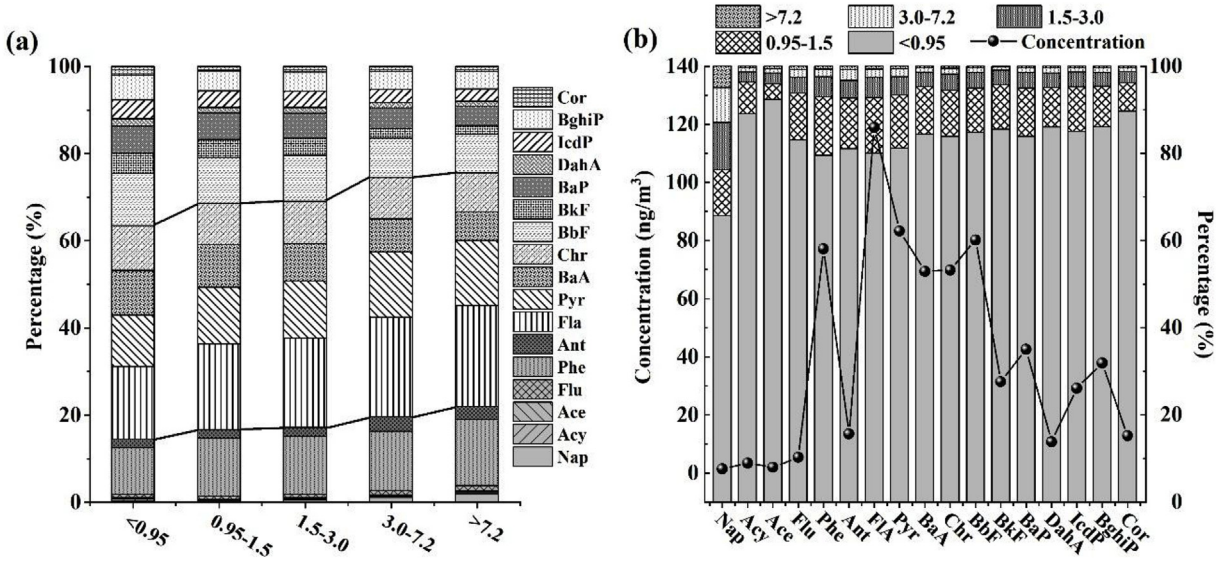

Fig. 4. (a) Compositions in percentages of PAHs in different size ranges; (b) the concentrations (ng/m^3) and fractioned size composition (%) of individual PAHs.

1.4 μm; low caking coals (0.95–0.98 μm) (Shen et al., 2010, 2013), indicating the combined pollution of these sources in Fenhe Plain. In addition, condensation mechanisms may also account for the low MMD values of the PAHs because the gas-particle condensation always enriches the aerosol fraction in the accumulation size range (0.05~2 μm) (Bi et al., 2005; Wu et al., 2006; Zhu et al., 2014).

3.3. The effect of meteorological parameters on the size distribution of PAHs

To have a clear knowledge about the influences of meteorological parameters on the size distribution, more analysis has been done. In the current work, there was a significantly negative correlation between the concentration of T-PAHs in each size range and wind speed (Table 1). This could be attributed to the role played by the wind in the pollutant dispersion. Wind can also influence the size distribution of PAHs as that we can observed on the days of Dec 15 and 30 in 2014 (Fig. 2a and b). On those two days, there were large increases in the proportion of $PM_{0.95}$-bound PAHs along with sharp increases in the wind speed compared with the previous day, while the temperature and humidity were almost unchanged. One possible reason is that good conditions for dispersion of aerosol decreased the percentage of coarser particles because we can also observe significant increases of the proportion of $PM_{0.95}$ simultaneously (Fig. 2c).

Table 1 showed that there was a significant correlation between humidity and PAHs in three particle size fractions including 0.95–1.5 μm, 1.5–3.0 μm and 3.0–7.2 μm. Humidity has an important influence on the growth of atmospheric particles due to the moisture absorption (Chrysikou and Samara, 2009). Our results indicate that a large part of the PAHs in the three particle size fractions were transferred from the finer particles during the growth process. Under stable weather conditions, the influence of humidity was more obvious. Take the period of Dec 23–27 in 2014 as an example, the temperature changed little and the wind speed was low, the proportion of particulate matter and PAHs in the size range of 0.95–7.2 μm showed an obvious increase accompanying with the continuous increase of the humidity (Fig. 2a–c). The PAHs in the size range of < 0.95 μm displayed an opposite trend. There was no statistically significant correlation between the humidity and T-PAHs in $PM_{0.95}$ and $PM_{7.2\text{-}10}$, indicating that the PAHs in the two size ranges were associated with particles initially emitted.

Although temperature can influence the vaporization and condensation of PAHs, none of the size ranges was observed in which the concentration of the total particulate PAHs has significant correlation with the temperature (Table 1). However, it is worth noting that when the local wind speed and temperature decreased sharply simultaneously on the day of Dec 31 in 2014, while the humidity kept stable, the distribution ratio of PAHs increased significantly in the size range of 0.95–7.2 μm (Fig. 2a and b). The possible reason is that the lower temperature and wind speed promoted the conversion of PAHs, especially low ring number PAHs, from gas phase into the particle phase.

3.4. Difference analysis of PAHs sources in different size ranges

To further identify the differences of the sources of PAHs in different size ranges, several diagnostic ratios including BaA/(BaA + Chr), Ant/(Ant + Phe), Fla/(Fla + Pyr), IcdP/(IcdP + BghiP) and Fla/Pyr were analyzed which were widely used in many source identification studies. A BaA/(BaA + Chr) ratio that is higher than 0.35 signals combustion sources (i.e., incomplete combustion of fossil fuels and plant material), lower than 0.2 indicates petrogenic sources (i.e., unburned fossil material such as crude oils, coal, fuel, or various refinery products), while between 0.2 and 0.35 indicates the mixture of petroleum and combustion sources (Zhu et al., 2014; Wang et al., 2016b). The Ant/(Ant + Phe) ratio greater than 0.1 signals combustion sources, less than 0.1 indicates petrogenic sources (Budzinski et al., 1997; Duan et al., 2007). The Fla/Pyr ratio higher than 1.0 signals combustion sources, while lower than 1.0 indicates petrogenic sources (Lee et al., 2005). The Fla/(Fla + Pyr) ratios < 0.4 are usually taken as an indication of petrogenic sources, > 0.5 implies coal/biomass combustion, and between 0.4 and 0.5 indicates traffic emissions (Alves et al., 2016; Wang et al., 2016b). The IcdP/(IcdP + BghiP) ratio is below 0.2 for petrogenic sources, above 0.5 for coal/biomass combustion, and ranges from 0.2 to 0.5 for traffic emissions (Shi et al., 2015; Wang et al., 2016b). In this study, the values of BaA/(BaA + Chr) in different size ranges varied from 0.41 to 0.51, Ant/(Ant + Phe) varied from 0.15 to 0.18, Fla/Pyr varied from 1.38 to 1.52, all of which indicate that combustion is the main source of PAHs in Fenhe Plain. Fla/(Fla + Pyr) ratios ranged from 0.58 to 0.60, and IcdP/(IcdP + BghiP) ratios ranged from 0.40 to 0.45, further suggesting coal combustion as the predominant source. The result is consistent with the fact that large amounts of coal are combusted for heating in winter of Fenhe Plain (Fig. 6).

Few differences were found in the molecular ratios of PAH components in different size ranges. To demonstrate if it implied that the PAHs bound to different size particles have similar sources, we further analyzed the similarities among the PAHs profiles in different sizes by applying the coefficient of divergence (CD) analysis. The detailed

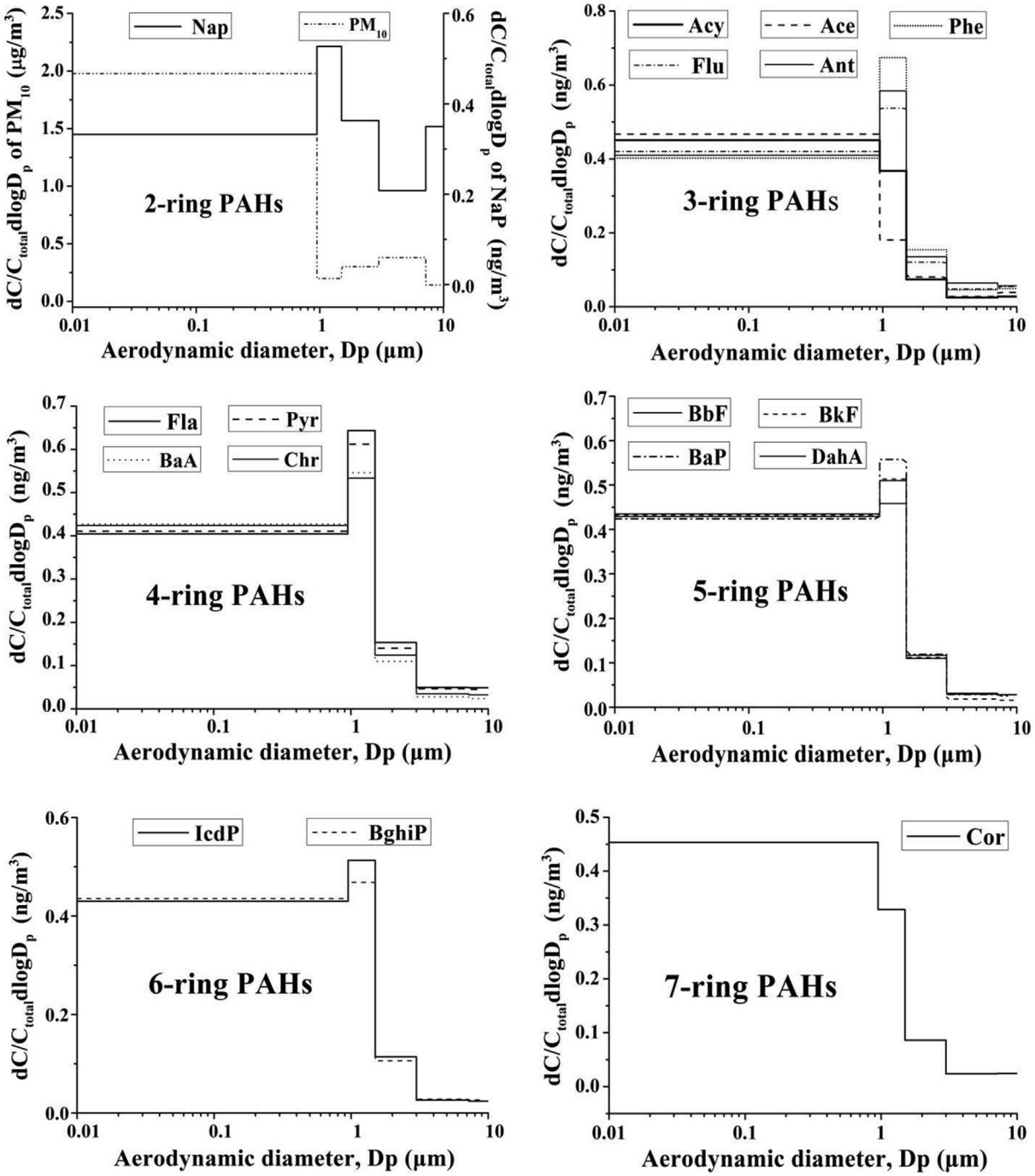

Fig. 5. Size distribution mode of individual PAHs. dC is the mass concentration on each filter, C is the sum concentration on all filters, and $dlogD_p$ is the logarithmic size interval for each impactor stage in aerodynamic diameter (D_p).

method has been reported in many other studies (He et al., 2014; Lv et al., 2016). The value less than 0.2 means that two PAHs profiles are influenced by common sources (Kong et al., 2012; He et al., 2014), while CD values larger than 0.2 indicate heterogeneous PAHs spatial distribution (Wilson et al., 2005; Lv et al., 2016). In the present study, the PAHs' CD diagrams distinguished by different colors are shown in Fig. 7. Interestingly, the CD values either between the adjacent sizes or between the nonadjacent sizes were all higher than 0.2, indicating that PAHs between all of the sizes had a high spatial heterogeneity in source factor contributions. The larger the difference between the compared sizes, the larger the CD value for them. Different conclusions given by the CD values from the molecular ratios of PAH components hint that molecular ratio analysis is a rough way to do the source analysis of PAHs. Our results also suggest that coagulation was not the main mechanism for PAHs associated with coarse particles, because if it was, the PAHs profiles in fine and coarse particles would be similar with a low CD value (Wu et al., 2006).

3.5. *The inhalation exposure and health risk evaluation of particulate PAHs*

From the results of PAHs distribution, we could see an important implication regarding health hazards from inhalation exposure. Since the majority of HMW PAHs have mutagenic and/or carcinogenic properties and almost exclusively exist on fine particles, these PAHs can

Table 1
Pearson correlation coefficients between the concentrations of T-PAHs in different size range of particles and meteorological parameters.

Size range	T	RH	WS	P
< 0.95 μm	0.308	0.295	−0.720**	0.291
0.95–1.5 μm	0.188	0.667**	−0.611**	0.231
1.5–3.0 μm	0.128	0.620**	−0.564**	0.222
3.0–7.2 μm	0.027	0.470*	−0.626**	0.278
7.2–10 μm	0.092	0.374	−0.644**	0.349
PM_{10}	0.291	0.395	−0.735**	0.296

T: Ambient temperature (°C); RH: Relative humidity (%); WS: Wind speed (m/s); and P: Pressure (kPa).
Correlation is significant at the 0.01 level.

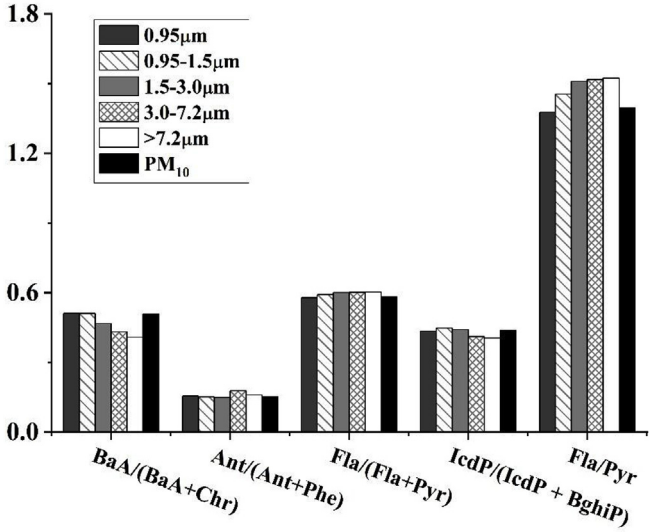

Fig. 6. Diagnostic molecular ratios of PAH components in particles of different size fractions.

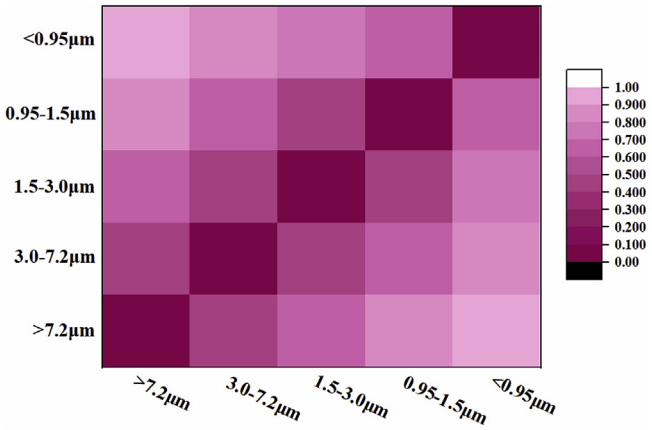

Fig. 7. Similarity comparisons of PAHs profiles for different particle fractions.

travel deep into the human respiratory system and hence can pose a serious health risk through exposing a person to both particles and the loaded carcinogenic PAHs (Kameda et al., 2005; Lv et al., 2016). Considering this, we further estimated the residential inhalation exposure situation to the outdoor size-fractioned particulate-bound PAHs in Fenhe Plain, and then evaluated the corresponding health risk.

The inhalation exposure level of PAHs was highly dependent on its particle size distribution (Luo et al., 2015). The calculated inhalable, thoracic, and respirable fractions of PAHs bound to PM_{10} were 98–99%, 98–99% and 96–98% in Fenhe Plain (Fig. 8a). This indicates that almost all particulate PAHs can be inhaled into the body. By comparison, those fractions in Guangzhou urban area (91–97%, 80–95% and 67–93%) and Qingyuan e-waste recycling zone (90–97%, 78–97% and 66–94%) of China were a bit lower (Luo et al., 2015). The high-efficiency inhalation of particulate PAHs in Fenhe Plain can be attributed to the very large proportion of ultrafine and fine particles. However, only 21–35% of particulate PAHs in Fenhe Plain could deposit in the human respiratory system with the average level being 25.78% (Fig. 8b), which is lower than that in Guangzhou (30%–50%) (Luo et al., 2015). This result is due to that many ultrafine particles can be exhaled out from human body easily although they could reach sites deep in the lungs (Hinds et al., 1999). Therefore, the particle size distribution must be considered in assessing the effect of particulate matters and the associated components on human health.

The deposition efficiency showed few differences among the individual PAH components in both the tracheobronchial and alveolar regions. However, in head region, the deposition efficiency of Nap was much higher than that of other PAHs, followed by Flu, Phe, Ant, Fla and Pyr, while the deposition efficiency of the rest individual components slightly decreased along with the increase of molecular weight (Fig. 8b). The deposition efficiency of particulate PAHs was highest in alveolar region (13.78%), followed by head region (9.13%) and tracheobronchial region (2.87%) (Fig. 8b). Correspondingly, the deposition flux of particulate PAHs in the three regions were 42.66, 30.50 and 9.00 ng/h (Fig. 8c). The total PAHs deposition flux (82.16 ng/h) is far higher than that in indoor air of the urban community of Guangzhou, China (3.7 ng/h) (Zhang et al., 2012), and urban atmosphere of Shanghai, China (8.8 ng/h) (Lv et al., 2016), but it is lower than that to which traffic police in Beijing are exposed (280 ng/h) at the respiratory rate of 0.83 m^3/h (Liu et al., 2007). The deposition site of the particle-bound PAHs in the respiratory tract was highly dependent on the particle size. The PAHs bound to $PM_{0.95}$ deposited predominantly in alveolar region, followed by tracheobronchial region. The deposition flux in head region was slightly lower than that in tracheobronchial region. On the contrary, the PAHs bound to $PM_{0.95\text{-}10}$ mainly deposited in head region, followed by alveolar region, while very few deposited in the tracheobronchial region.

The PAHs deposited in respiratory system, especially in the alveolar region, can be rapidly transferred into blood system and spread throughout the body, resulting hazards for human health. Therefore, incremental lifetime cancer risk of the deposited PAHs of the human respiratory system was estimated. The results showed that the average estimated incremental lifetime cancer risk in PM_{10} were as high as 1693.76 cancer cases per million people (Fig. 8d). According to the official data reported by Shanxi provincial people's hospital, lung cancer is the top 1 cancer in Shanxi with the incidence rate being as high as 1/1000, which is twice of the national average (SPPH, 2016). The roles of PAHs cannot be ignored. Our study suggests that atmospheric PAHs pollution should be controlled seriously to prevent the residential people from lung cancer. The contribution of < 0.95 μm size fraction contributed the most to the total cancer risk, reaching up to 62.44%. The contributions of the rest four particle size fractions were 21.34%, 10.84%, 4.10% and 1.29% in an increasing order of particle size, respectively (Fig. 8d). Although the main components of the PAHs in PM_{10} in Fenhe Plain were Phe, Fla, Pyr, BaA, Chr and BbF (Fig. 4b), the major carcinogenic components were BaP, DahA, BbF, BaA, BkF and IcdP in the 17 investigated PAHs. Their contribution to the total cancer risk accounted for 56.53%, 13.91%, 10.53%, 9.13%, 4.05% and 3.81%, respectively (Fig. 8d).

To have a clear knowledge about the detailed sources of the above six carcinogenic components, we run the positive matrix factorization (PMF) model again through the same method we have reported in a previous study (Li et al., 2016). The data we used is the incorporation of the two studies which were conducted at the same sampling site, because the sample number of this study can't satisfy the model requirement. The detailed data information and boundary conditions for the

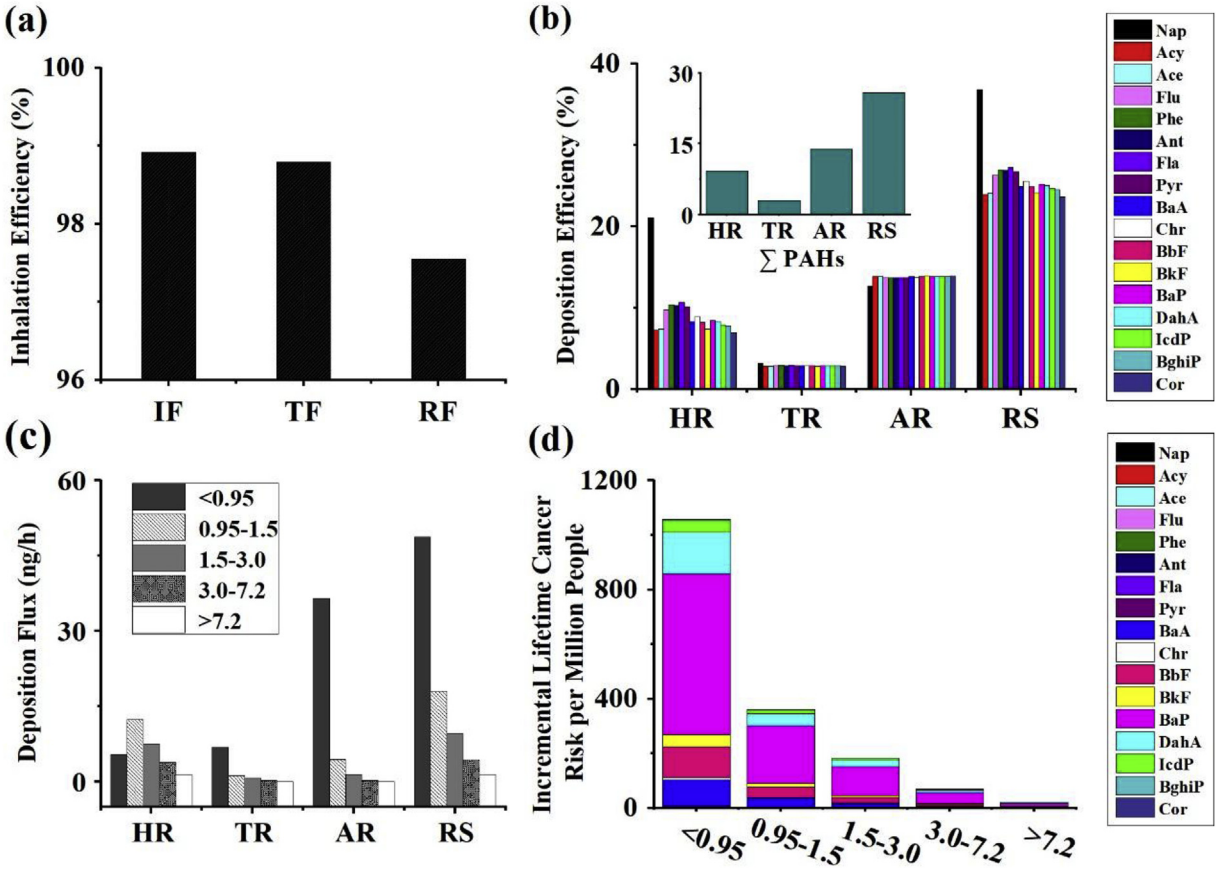

Fig. 8. (a) The inhalation efficiency (%) of PM_{10}-bound PAHs entering into different regions of the human respiratory system (IF, inhalable fraction; TF, thoracic fraction; RF, respirable fraction); (b) The deposition efficiency (%) of PM_{10}-bound individual PAHs in different regions of the human respiratory system (HR, the head region; TR, tracheobronchial region; AR, alveolar region; RS, the total respiratory system); (c) The deposition fluxes (ng/h) of particle size-fractionated PAHs in different regions of the human respiratory system; (d) Estimated incremental lifetime cancer risk of particle size-fractionated PAHs for residents in Taiyuan based on deposition concentrations.

analysis being performed was introduced in the supplementary materials (Text S2). We find that the factor profiles haven't too much change (Fig. S3), but the contribution of coking and coal combustion has decreased, while that of the traffic exhausts has a large increase from 20% to 27% (Figs. S4 and S5). The traffic exhaust has the largest contribution to five of the major carcinogenic components-BaP, DahA, BbF, BaA and IcdP, accounting for 68%, 95%, 65%, 56% and 84%, respectively. For BaP, BbF, BaA and IcdP, coal combustion also has remarkable contributions, about 30%, 23%, 31% and 10%, respectively. Coal combustion contributes the most to BkF (47%), followed by traffic exhausts (30%). Coking activity has significant contributions to BbF, BaA and BkF, about 12%, 13% and 23%, respectively (Fig. 9).

4. Summary

In this study, health cancer risk of particulate PAHs and the major sources of the main carcinogenic components were explored based on the analysis of the concentration level, composition and size distribution in winter in Fenhe Plain. The results showed that the average mass concentration of PM_{10} bound PAHs was 689.19 ng/m^3, which is higher than that in many other domestic and foreign cities. The < 0.95 μm size range had an extremely high contribution to the total PAHs in PM_{10}, and the MMD values were very low for both PM_{10} and the associated PAHs, indicating a serious fine particle pollution in this region. Except for Nap which exhibited a bimodal distribution, the remaining individual PAHs all followed a nearly unimodal size distribution with the peak locating in the accumulation fraction. The distribution pattern of the particulate PAHs is closer to that of emission sources than the urban atmosphere in many other places. This indicates that particulate PAHs are mainly from local emissions. In addition, the low temperature and dry environment don't favor the redistribution of PAHs in different size particles.

Our study finds that the distribution of PM_{10} is not the controlling factor of the PAHs size distribution in the winter of Fenhe Plain, while wind speed and humidity has significant influence on it. Although the diagnostic ratios were considered as a convenient method for identifying possible emission sources by many studies, it is hard to distinguish the sources of PAHs in nonadjacent particles. CD analysis indicates that PAHs between all of the sizes had a high spatial heterogeneity in source factor contributions. Condensation is probably an important mechanism for PAHs size distribution but not the coagulation.

Respiratory exposure assessment finds that more than 98% of PM_{10}-PAHs can enter the human respiratory tract, of which more than 96% can reach the alveolar. But only 21–35% of the particulate could deposit in the respiratory system. The incremental lifetime cancer risk of inhalation exposure to particulate PAHs in Fenhe Plain was 1693.76 cases per million people. But this risk has not yet included the health risk of gas phase PAHs. This indicates that the pollution situation of PAHs in winter of Fenhe Plain is very serious, which poses a serious threat to the health of the local residents. The contribution of < 0.95 μm particles to the total cancer risk is the largest, which is up to 62.44%. The major cancer risk contributors, including BaP, DahA, BbF, BaA, BkF and IcdP, are mainly emitted from vehicles exhausts and coal combustion. The contribution of coal combustion has decreased, but the contribution of traffic exhausts has an increase of beyond 7% compared with the years before this study. Therefore, stringent

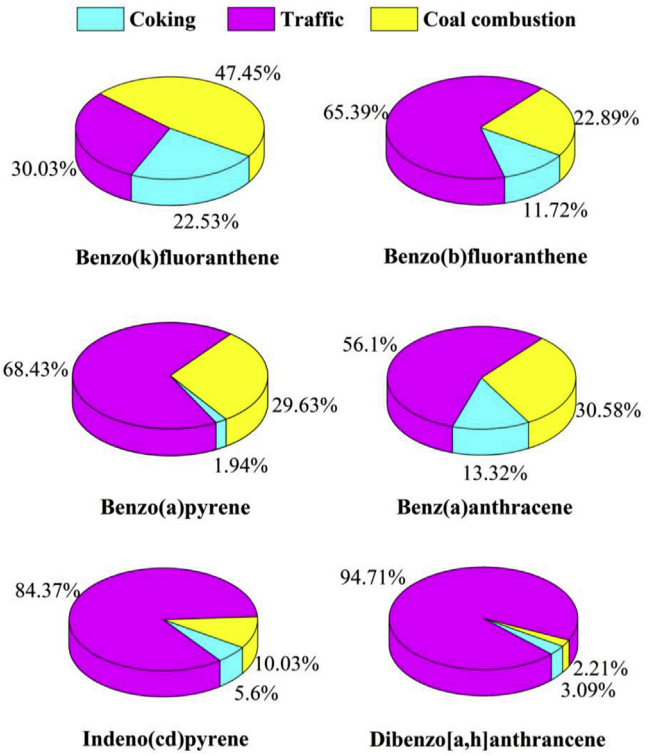

Fig. 9. Source contributions to the major carcinogenic components (BkF, BbF, BaP, BaA, IcdP and DahA) resolved by PMF.

restrictive measures on the traffic activity should be implemented as soon as possible by the local authority of Fenhe Plain to protect the health of local residents.

Declaration of competing interest

The authors declare that they have no known competing financial interests or personal relationships that could have appeared to influence the work reported in this paper.

Acknowledgements

The work was funded by the National Natural Science Foundation of China (No. 41501543, 41472311), the Shanxi Province Key Program for International Science and Technology Cooperation Projects (201803D421095), the Shanxi Province Science Foundation for Youths (No. 2015021059) and the Special Scientific Research Funds for Environmental Protection Commonwealth Section (20603020802L). The authors duly acknowledge the partial support received from the One-hundred Talent Program, which was supported by the Organization Department of Shanxi Province Committee.

Appendix A. Supplementary data

Supplementary data to this article can be found online at https://doi.org/10.1016/j.atmosenv.2019.116924.

References

Akyüz, M., Çabuk, H., 2009. Meteorological variations of $PM_{2.5}/PM_{10}$ concentrations and particle-associated polycyclic aromatic hydrocarbons in the atmospheric environment of Zonguldak, Turkey. J. Hazard Mater. 170, 13–21. https://doi.org/10.1016/j.jhazmat.2009.05.029.

Amarillo, A.C., Mateos, A.C., Carreras, H., 2017. Source apportionment of PM_{10}-bound polycyclic aromatic hydrocarbons by positive matrix factorization in Córdoba city, Argentina. Arch. Environ. Contam. Toxicol. 72, 380–390. https://doi.org/10.1007/s00244-017-0384-y.

Alves, C.A., Vicente, A.M.P., Gomes, J., Nunes, T., Duarte, M., Bandowe, B.A.M., 2016. Polycyclic aromatic hydrocarbons (PAHs) and their derivatives (oxygenated-PAHs, nitrated-PAHs and azaarenes) in size-fractionated particles emitted in an urban road tunnel. Atmos. Res. 180, 128–137. https://doi.org/10.1016/j.atmosres.2016.05.013.

Bi, X., Sheng, G., Peng, P., Chen, Y., Fu, J., 2005. Size distribution of n-alkanes and polycyclic aromatic hydrocarbons (PAHs) in urban and rural atmospheres of Guangzhou, China. Atmos. Environ. Times 39, 477–487. https://doi.org/10.1016/j.atmosenv.2004.09.052.

Boström, C.E., Gerde, P., Hanberg, A., Jernström, B., Johansson, C., Kyrklund, T., Rannug, A., Törnqvist, M., Victorin, K., Westerholm, R., 2002. Cancer risk assessment, indicators, and guidelines for polycyclic aromatic hydrocarbons in the ambient air. Environ. Health Perspect. 110, 451–489. http://ehpnet1.niehs.nih.gov/docs/2002/suppl-3/451-489bostrom/abstract.html.

Bourotte, C., Forti, M.C., Taniguchi, S., Bícego, M.C., Lotufo, P.A., 2005. A wintertime study of PAHs in fine and coarse aerosols in São Paulo city, Brazil. Atmos. Environ. 39, 3799–3811. https://doi.org/10.1016/j.atmosenv.2005.02.054.

Budzinski, H., Jones, I., Bellocq, J., Pierard, C., Garrigues, P.H., 1997. Evaluation of sediment contamination by polycyclic aromatic hydrocarbons in the Gironde estuary. Mar. Chem. 58, 85–97. https://doi.org/10.1016/S0304-4203(97)00028-5.

Chrysikou, L.P., Samara, C.A., 2009. Seasonal variation of the size distribution of urban particulate matter and associated organic pollutants in the ambient air. Atmos. Environ. 43, 4557–4569. https://doi.org/10.1016/j.atmosenv.2009.06.033.

Di Vaio, P., Cocozziello, B., Corvino, A., Fiorino, F., Frecentese, F., Magli, E., Onorati, G., Saccone, I., Santagada, V., Settimo, G., Severino, B., Perissutti, E., 2016. Level, potential sources of polycyclic aromatic hydrocarbons (PAHs) in particulate matter (PM_{10}) in Naples. Atmos. Environ. 129, 186–196. https://doi.org/10.1016/j.atmosenv.2016.01.020.

Duan, J., Bi, X., Tan, J., Sheng, G., Fu, J., 2007. Seasonal variation on size distribution and concentration of PAHs in Guangzhou city, China. Chemosphere 67, 614–622. https://doi.org/10.1016/j.chemosphere.2006.08.030.

Duan, J., Tan, J., Wang, S., Chai, F., He, K., Hao, J., 2012. Roadside, Urban, and Rural comparison of size distribution characteristics of PAHs and carbonaceous components of Beijing, China. J. Atmos. Chem. 69, 337–349. https://doi.org/10.1007/s10874-012-9242-5.

Geiser, M., Rothen-Rutishauser, B., Kapp, N., Schurch, S., Kreyling, W., Schulz, H., Semmler, M., Hof, V.I., Heyder, J., Gehr, P., 2005. Ultrafine particles cross cellular membranes by nonphagocytic mechanisms in lungs and in cultured cells. Environ. Health Perspect. 113, 1555–1560. https://doi.org/10.1289/ehp.8006.

He, J., Fan, S., Meng, Q., Sun, Y., Zhang, J., Zu, F., 2014. Polycyclic aromatic hydrocarbons (PAHs) associated with fine particulate matters in Nanjing, China: distributions, sources and meteorological influences. Atmos. Environ. 89, 207–215. https://doi.org/10.1016/j.atmosenv.2014.02.042.

Hien, T.T., Thanh, L.T., Kameda, T., Takenaka, N., Bandow, H., 2007. Distribution characteristics of polycyclic aromatic hydrocarbons with particle size in urban aerosols at the roadside in Ho Chi Minh City, Vietnam. Atmos. Environ. Times 41, 1575–1586. https://doi.org/10.1016/j.atmosenv.2006.10.045.

Hinds, W.C., 1999. Aerosol Technology: Properties, Behavior, and Measurement of Airborne Particles, second ed. Wiley Interscience, New York.

Hong, H., Yin, H., Wang, X., Ye, C., 2007. Seasonal variation of PM_{10}-bound PAHs in the atmosphere of Xiamen, China. Atmos. Res. 85, 429–441. https://doi.org/10.1016/j.atmosres.2007.03.004.

Hoseini, M., Yunesian, M., Nabizadeh, R., Yaghmaeian, K., Ahmadkhaniha, R., Rastkari, N., Parmy, S., Faridi, S., Rafiee, A., Naddafi, K., 2016. Characterization and risk assessment of polycyclic aromatic hydrocarbons (PAHs) in urban atmospheric Particulate of Tehran, Iran. Environ. Sci. Pollut. Res. 23, 1820–1832. https://doi.org/10.1007/s11356-015-5355-0.

International Commission on Radiological Protection, 1994. Publication 66: human respiratory tract model for radiological protection. Ann. ICRP 24 (1–3).

Jiang, Q., Li, Y., Hu, X., Lu, B., Tao, S., Wang, R., 2013. Estimation of annual emission and distribution characteristics of polycyclic aromatic hydrocarbons (PAHs) in Taiyuan. China Environ. Sci. 33, 14–20. https://doi.org/10.3969/j.issn.1000-6923.2013.01.003.

Kameda, Y., Shirai, J., Komai, T., Nakanishi, J., Masunaga, S., 2005. Atmospheric polycyclic aromatic hydrocarbons: size distribution, estimation of their risk and their depositions to the human respiratory tract. Sci. Total Environ. 340, 71–80. https://doi.org/10.1016/j.scitotenv.2004.08.009.

Kaupp, H., McLachlan S., M., 1999. Atmospheric particle size distributions of polychlorinated dibenzo-p-dioxins and dibenzofurans (PCDD/Fs) and polycyclic aromatic hydrocarbons (PAHs) and their implications for wet and dry deposition. Atmos. Environ. 33, 85–95. https://doi.org/10.1016/S1352-2310(98)00129-0.

Kaur, S., Senthilkumar, K., Verma, V.K., Kumar, B., Kumar, S., Katnoria, J.K., Sharma, C.S., 2013. Preliminary analysis of polycyclic aromatic hydrocarbons in air particles (PM_{10}) in Amritsar, India: sources, apportionment and possible risk implications to humans. Arch. Environ. Contam. Toxicol. 65, 382–395. https://doi.org/10.1007/s00244-013-9912-6.

Kavouras, I.G., Stephanou, E.G., 2002. Particle size distribution of organic primary and secondary aerosol constituents in urban, background marine, and forest atmosphere. J. Geophys. Res. 107 (D8). https://doi.org/10.1029/2000JD000278.

Keshtkar, H., Ashbaugh, L.L., 2007. Size distribution of polycyclic aromatic hydrocarbon particulate emission factors from agricultural burning. Atmos. Environ. 41, 2729–2739. https://doi.org/10.1016/j.atmosenv.2006.11.043.

Kong, S., Ding, X., Bai, Z., Han, B., Chen, L., Shi, J., Li, Z., 2010. A seasonal study of polycyclic aromatic hydrocarbons in $PM_{2.5}$ and $PM_{2.5-10}$ in five typical cities of Liaoning Province, China. J. Hazard Mater. 183, 70–80. https://doi.org/10.1016/j.jhazmat.2010.06.107.

Kong, S., Lu, B., Ji, Y., Bai, Z., Xu, Y., Liu, Y., Jiang, H., 2012. Distribution and sources of polycyclic aromatic hydrocarbons in size differentiated re-suspended dust on building surfaces in an oilfield city, China. Atmos. Environ. 55, 7–16. https://doi.org/10.1016/j.atmosenv.2012.03.044.

Lee, B.C., Shimizu, Y., Matsuda, T., Matsui, S., 2005. Characterization of polycyclic aromatic hydrocarbons (PAHs) in different size fractions in deposited road particles (DRPs) from Lake Biwa area, Japan. Environ. Sci. Technol. 39, 7402–7409. https://doi.org/10.1021/es050103n.

Li, H., Guo, L., Cao, R., Gao, B., Yan, Y., He, Q., 2016. A wintertime study of $PM_{2.5}$-bound polycyclic aromatic hydrocarbons in Taiyuan during 2009–2013: assessment of pollution control strategy in a typical basin region. Atmos. Environ. 140, 404–414. https://doi.org/10.1016/j.atmosenv.2016.06.013.

Li, Z., Ren, A., Zhang, L., Ye, R., Li, S., Zheng, J., Hong, S., Wang, T., Li, Z., 2006. Extremely high prevalence of neural tube defects in a 4-county area in Shanxi Province, China. Birth Defects Res. Part A Clin. Mol. Teratol. 76, 237–240. https://doi.org/10.1002/bdra.20248.

Lin, C.C., Chen, S.J., Huang, K.L., Lee, W.J., Tsai, J.H., Chaung, H.C., 2008. PAHs, PAH-induced carcinogenic potency, and particle-extract-induced cytotoxicity of traffic-related nano/ultrafine particles. Environ. Sci. Technol. 42, 4229–4235. https://doi.org/10.1021/es703107w.

Liu, X., Peng, L., Bai, H., Mu, L., Song, C., 2014. Occurrence and particle-size distributions of polycyclic aromatic hydrocarbons in the ambient air of coking plant. Environ. Geochem. Health 36, 531–542. https://doi.org/10.1007/s10653-013-9579-y.

Liu, Y.N., Tao, S., Dou, H., Zhang, T.W., Zhang, X.L., Dawson, R., 2007. Exposure of traffic police to polycyclic aromatic hydrocarbons in Beijing, China. Chemosphere 66, 1922–1928. https://doi.org/10.1016/j.chemosphere.2006.07.076.

Luo, P., Bao, L.J., Li, S.M., Zeng, E.Y., 2015. Size-dependent distribution and inhalation cancer risk of particle-bound polycyclic aromatic hydrocarbons at a typical e-waste recycling and an urban site. Environ. Pollut. 200, 10–15. https://doi.org/10.1016/j.envpol.2015.02.007.

Lv, Y., Li, X., Xu, T.T., Cheng, T.T., Yang, X., Chen, J.M., Iinuma, Y., Herrmann, H., 2016. Size distributions of polycyclic aromatic hydrocarbons in urban atmosphere: sorption mechanism and source contributions to respiratory deposition. Atmos. Chem. Phys. 16, 2971–2983. https://doi.org/10.5194/acp-16-2971-2016.

MEP (Ministry of Environmental Protection, China), 2012. Ambient air quality standards (GB 3095-2012). http://kjs.mep.gov.cn/hjbhbz/bzwb/dqhjbh/dqhjzlbz/201203/W020120410330232398521.pdf.

Mu, L., Peng, L., Liu, X., He, Q., Bai, H., Yan, Y., Li, Y., 2017. Emission characteristics and size distribution of polycyclic aromatic hydrocarbons from coke production in China. Atmos. Res. 197, 113–120. https://doi.org/10.1016/j.atmosres.2017.06.028.

Omar, N.Y.M.J., Abas, M.R.B., Ketuly, K.A., Tahir, N.M., 2002. Concentrations of PAHs in atmospheric particles (PM_{10}) and roadside soil particles collected in Kuala Lumpur, Malaysia. Atmos. Environ. 36, 247–254. https://doi.org/10.1016/S1352-2310(01)00425-3.

Ren, A., Qiu, X., Jin, L., Ma, J., Li, Z., Zhang, L., Zhu, H., Finnell, R.H., Zhu, T., 2011. Association of selected persistent organic pollutants in the placenta with the risk of neural tube defects. Proc. Natl. Acad. Sci. U.S.A. 108, 12770–12775. https://doi.org/10.1073/pnas.1105209108.

Ren, Y., Zhou, B., Tao, J., Cao, J., Zhang, Z., Wu, C., Wang, J., Li, J., Zhang, L., Han, Y., Liu, L., Cao, C., Wang, G., 2017. Composition and size distribution of airborne particulate PAHs and oxygenated PAHs in two Chinese megacities. Atmos. Res. 183, 322–330. https://doi.org/10.1016/j.atmosres.2016.09.015.

Saarnio, K., Sillanpää, M., Hillamo, R., Sandell, E., Pennanen, A.S., Salonen, R.O., 2008. Polycyclic aromatic hydrocarbons in size-segregated particulate matter from six urban sites in Europe. Atmos. Environ. 42, 9087–9097. https://doi.org/10.1016/j.atmosenv.2008.09.022.

SPPH (Shanxi Provincial People's Hospital), 2016. The foundation ceremony of the lung nodule diagnosis and treatment sub-center and the academic seminar of multi-disciplinary comprehensive treatment of lung cancer in Shanxi provincial people's hospital [DB/OL]. http://www.sxsrmyy.com/ksjs/tindex_ks.asp?id=1090&ksbh=15&lmbh=2.

Sharma, H., Jain, V.K., Khan, Z.H., 2008. Atmospheric polycyclic aromatic hydrocarbons (PAHs) in the urban air of Delhi during 2003. Environ. Monit. Assess. 147, 43–55. https://doi.org/10.1007/s10661-007-0096-2.

Shen, G., Wang, W., Yang, Y., Zhu, C., Min, Y., Xue, M., Ding, J., Li, W., Wang, B., Shen, H., Wang, R., Wang, X., Tao, S., 2010a. Emission factors and particulate matter size distribution of polycyclic aromatic hydrocarbons from residential coal combustions in rural Northern China. Atmos. Environ. 44, 5237–5243. https://doi.org/10.1016/j.atmosenv.2010.08.042.

Shen, G., Wei, S., Zhang, Y., Wang, B., Wang, R., Shen, H., Li, W., Huang, Y., Chen, Y., Chen, H., Tao, S., 2013. Emission and size distribution of particle-bound polycyclic aromatic hydrocarbons from residential wood combustion in rural China. Biomass Bioenergy 55, 141–147. https://doi.org/10.1016/j.biombioe.2013.01.031.

Shen, G., Yang, Y., Wang, W., Tao, S., Zhu, C., Min, Y., Xue, M., Ding, J., Wang, B., Wang, R., Shen, H., Li, W., Wang, X., Russell, A.G., 2010b. Emission factors of particulate matter and elemental carbon for crop residues and coals burned in typical household stoves in China. Environ. Sci. Technol. 44, 7157–7162. https://doi.org/10.1021/es101313y.

Shi, G.L., Zhou, X.Y., Jiang, S.Y., Tian, Y.Z., Liu, G.R., Feng, Y.C., Chen, G., Liang, Y.K.X., 2015. Further insights into the composition, source, and toxicity of PAHs in size-resolved particulate matter in a megacity in China. Environ. Toxicol. Chem. 34, 480–487. https://doi.org/10.1002/etc.2809.

Theodosi, C., Grivas, G., Zarmpas, P., Chaloulakou, A., Mihalopoulos, N., 2011. Mass and chemical composition of size-segregated aerosols (PM_1, $PM_{2.5}$, PM_{10}) over Athens, Greece: local versus regional sources. Atmos. Chem. Phys. 11, 11895–11911. https://doi.org/10.5194/acp-11-11895-2011.

Tomaz, S., Shahpoury, P., Jaffrezo, J.L., Lammel, G., Perraudin, E., Villenave, E., Albinet, A., 2016. One-year study of polycyclic aromatic compounds at an urban site in Grenoble (France): seasonal variations, gas/particle partitioning and cancer risk estimation. Sci. Total Environ. 565, 1071–1083. https://doi.org/10.1016/j.scitotenv.2016.05.137.

Venkataraman, C., Friedlander, S.K., 1994. Size distributions of polycyclic aromatic hydrocarbons and elemental carbon. 2. Ambient measurements and effects of atmospheric processes. Environ. Sci. Technol. 28, 563–572. https://doi.org/10.1021/es00053a006.

Wang, F., Meng, D., Li, X., Tan, J., 2016a. Indoor-outdoor relationships of $PM_{2.5}$ in four residential dwellings in winter in the Yangtze River Delta, China. Environ. Pollut. 215, 280–289. https://doi.org/10.1016/j.envpol.2016.05.023.

Wang, J., Li, X., Jiang, N., Zhang, W., Zhang, R., Tang, X., 2015. Long term observations of $PM_{2.5}$-associated PAHs: comparisons between normal and episode days. Atmos. Environ. 104, 228–236. https://doi.org/10.1016/j.atmosenv.2015.01.026.

Wang, Q., Kobayashi, K., Wang, W., Ruan, J., Nakajima, D., Yagishita, M., Lu, S., Zhang, W., Suzuki, M., Saitou, T., Sekiguchi, K., Sankoda, K., Takao, Y., Nagae, M., Terasaki, M., 2016b. Size distribution and sources of 37 toxic species of particulate polycyclic aromatic hydrocarbons during summer and winter in Baoshan suburban area of Shanghai, China. Sci. Total Environ. 566, 1519–1534. https://doi.org/10.1016/j.scitotenv.2016.06.039.

Wang, W., Simonich, S., Giri, B., Chang, Y., Zhang, Y., Jia, Y., Tao, S., Wang, R., Wang, B., Li, W., Cao, J., Lu, X., 2011. Atmospheric concentrations and air–soil gas exchange of polycyclic aromatic hydrocarbons (PAHs) in remote, rural village and urban areas of Beijing-Tianjin region, North China. Sci. Total Environ. 409, 2942–2950. https://doi.org/10.1016/j.scitotenv.2011.04.021.

Whitby, K.T., Husar, R.B., Liu, B.Y.H., 1972. The aerosols size distribution of the Los Angeles smog. Aerosol Atmos. Chem. 237–264. https://doi.org/10.1016/B978-0-12-347250-2.50025-2.

Wilson, J.G., Kingham, S., Pearce, J., Sturman, A.P., 2005. A review of intraurban variations in particulate air pollution: implications for epidemiological research. Atmos. Environ. 39, 6444–6462. https://doi.org/10.1016/j.atmosenv.2005.07.030.

World Health Organization (WHO), 2000. Air Quality Guidelines for Europe Regional Office for Europe, second ed. World Health Organization, Copenhagen.

Wu, D., Wang, Z., Chen, J., Kong, S., Fu, X., Deng, H., Shao, G., Wu, G., 2014. Polycyclic aromatic hydrocarbons (PAHs) in atmospheric $PM_{2.5}$ and PM_{10} at a coal-based industrial city: implication for PAH control at industrial agglomeration regions, China. Atmos. Res. 149, 217–229. https://doi.org/10.1016/j.atmosres.2014.06.012.

Wu, S.P., Tao, S., Liu, W.X., 2006. Particle size distributions of polycyclic aromatic hydrocarbons in rural and urban atmosphere of Tianjin, China. Chemosphere 62, 357–367. https://doi.org/10.1016/j.chemosphere.2005.04.101.

Yang, H.H., Chien, S.M., Chao, M.R., Lin, C.C., 2005. Particle size distribution of polycyclic aromatic hydrocarbons in motorcycle exhaust emissions. J. Hazard Mater. 125, 154–159. https://doi.org/10.1016/j.jhazmat.2005.05.019.

Yu, Y.J., Yang, L., Li, L.Z., Wang, Q., Zhang, Y.P., Xiang, M.D., He, Y., Sun, P., 2013. Health risk assessments of heavy metals and PAHs bound to PM_{10} in Lanzhou city. Acta Sci. Circumstantiae 33, 2920–2927. https://doi.org/10.13671/j.hjkxxb.2013.11.011.

Zhang, K., Zhang, B.Z., Li, S.M., Wong, C.S., Zeng, E.Y., 2012. Calculated respiratory exposure to indoor size-fractioned polycyclic aromatic hydrocarbons in an urban environment. Sci. Total Environ. 431, 245–251. https://doi.org/10.1016/j.scitotenv.2012.05.059.

Zhang, Y., Lin, Y., Cai, J., Liu, Y., Hong, L., Qin, M., Zhao, Y., Ma, J., Wang, X., Zhu, T., Qiu, X., Zheng, M., 2016. Atmospheric PAHs in North China: spatial distribution and sources. Sci. Total Environ. 565, 994–1000. https://doi.org/10.1016/j.scitotenv.2016.05.104.

Zhang, Y., Shen, H., Tao, S., Ma, J., 2011. Modeling the atmospheric transport and outflow of polycyclic aromatic hydrocarbons emitted from China. Atmos. Environ. 45, 2820–2827. https://doi.org/10.1016/j.atmosenv.2011.03.006.

Zhang, Y., Tao, S., Cao, J., Coveney, R.M., 2007. Emission of polycyclic aromatic hydrocarbons in China by county. Environ. Sci. Technol. 41, 683–687. https://doi.org/10.1021/es061545h.

Zhang, Y., Tao, S., Shen, H., Ma, J., 2009. Inhalation exposure to ambient polycyclic aromatic hydrocarbons and lung cancer risk of Chinese population. Proc. Natl. Acad. Sci. U.S.A. 106, 21063–21067. https://doi.org/10.1073/pnas.0905756106.

Zhao, L., Chen, C., Wang, P., Chen, Z., Cao, S., Wang, Q., Xie, G., Wan, Y., Wang, Y., Lu, B., 2015. Influence of atmospheric fine particulate matter ($PM_{2.5}$) pollution on indoor environment during winter in Beijing. Build. Environ. 87, 283–291. https://doi.org/10.1016/j.buildenv.2015.02.008.

Zhou, J., Wang, T., Huang, Y., Mao, T., Zhong, N., 2005. Size distribution of polycyclic aromatic hydrocarbons in urban and suburban sites of Beijing, China. Chemosphere 61, 792–799. https://doi.org/10.1016/j.chemosphere.2005.04.002.

Zhu, Y., Yang, L., Yuan, Q., Yan, C., Dong, C., Meng, C., Sui, X., Yao, L., Yang, F., Lu, Y., Wang, W., 2014. Airborne particulate polycyclic aromatic hydrocarbon (PAH) pollution in a background site in the North China Plain: concentration, size distribution, toxicity and sources. Sci. Total Environ. 466, 357–368. https://doi.org/10.1016/j.scitotenv.2013.07.030.